TWO KINDS OF VARIANT IN SHAPE MEMORY MATERIAL①

Lin,Guangming Lai,J L② Huan,Yuanshi
Zhongshan University,Guangzhou 510275, China

ABSTRACT

In shape memory materials, that have been trained to have a two way shape memory effect (TWSM), the martensitic variants are classified into two groups, i.e., preferentially oriented variants and self-accommodating variants. Applied stress may promote or constrain the transition of preferentially oriented variants and so change transformation temperatures but has no essential effect on self-accommodating variants. According to the point of view mentioned above, some experimental phenomena during thermocycling of a TWSM device may be explained, such as the absence of synchronization between the plot of resistance change, temperature and the plot of memory strain vs. temperature.

Key words: shape memory alloy martensitic variant transformation constraint heating phase interface.

1 INTRODUCTION

Shape memory alloys are frequently used as a driving element for various actuators and working media for heat engines exploiting low-grade thermal reservoirs. Since the memory elements are subjected to the actions of outer load and temperature during operation, from the view of engineering, it is necessary to understand the effects of constraint heating on the shape memory properties such as shape recovery temperature[1-3], reversion stress[4], shape deterioration[5], hysteresis[6,7]and even transformation enthalpy[8].

It should be pointed out, the materials used for making shape memory elements usually are subjected to training processes[9] to produce TWME. The special features of these materials are preferential martensite reorientation and the development of reversible macro-shape recovery. We define this kind of material as shape memory material to distinguish it from thermoelastic martensite materials which have not been subjected to training.

There have been only a limited number of investigations on the transformation mechanism of shape memory materials under constraint conditions. Dunstan and kettley *et al* [1-2]studied the retarding effect of constrained stress on single direction shape recovery of nitinol wire and they suggested that this behaviour was a consequence of the constraint impeding for the motion of the interfaces. They also assumed that the shape recovery temperature and thermoelastic martensitic transformation temperature were identical, but this link has not yet been proven. One of the authors has studied the effect of stress on the transformation of a shape memory spring[3,10]The reults show that, when applied stress and variant shear (corresponding to macro-shape strain) have the same sign, the stress will promote the transformation and increase the transition starting temperature. Otherwise the stress will constrain the transformation and decrease the transition starting temperature. By using this effect, the

①Manuscript received Nov.5, 1992;
②Department of Applied Science, City Polytechnic of Hong Kong, Tat Chee Ave.,Kowloon, Hong Kong

snap-acting thermoelstic martensite transformation and snap-acting TWME effect can be obtained.

In this paper, we prove by using measurements of shape change ($\triangle L$) and resistance change ($\triangle R$) together with X−ray diffraction, there are two kinds of variants in shape memory materials, i.e., variant not concerned with macro-shape changes and variant concerned with shape change. The different response of two kinds of variant to the applied stress are also studied. The results have been explained according the transformation thermodynamic of a shape memory material under constraint heating.

2 EXPERIMENTAL PROCEDURES

Cu−Zn−Al alloy springs coiled from a 66.5 Cu−24.5 Zn−9.0 Al (at.−%) alloy wire were used as specimens for this study. The springs' specifications were: spring 1, diameter of alloy wire $d=2$ mm, internal diameter $\varphi=10$ mm, effective number of turns $n=7$ and initial length $L_0=20$ mm; spring 2, $d=3$ mm, $\varphi=5$ mm, $n=5$, and $L_0=15$ mm. Both spring were subjected to constrained thermocyclic training before the experiment. The spring specimens showed stable TWSM at a temperature range from 283 K to 333 K, i.e., the spring extended with increasing temperature and shortened with decreasing temperature. The maximum TWSM extensions ($\triangle L_m$) were 20 mm and 8 mm for spring 1 and spring 2 respectively.

The length change ($\triangle L$), and electrical resistance change ($\triangle R$) of the spring were measured simultaneously as a function of temperature (T) under a compression load. $\triangle L$ was measured by an extensometer, $\triangle R$ by a digital micro-ohmmeter and T by a copper-constantan thermocouple welded onto the specimen. The signals were input into a high-precision X−Y recorder for generating the hysteresis loops. The temperature change, at a rate of about 5 degrees Kelvin per minute, was achieved by a water bath with heating and cooling elements.

X−ray diffraction was carried out using a Kigaku $D/$MAX IIIA diffractometer. Cu K_α radiation was used, and the 2θ scanning rate was set at 2(°)/min. Temperature variation was provided by blowing hot air over the sample, which could be restrained mechanically by a jig.

3 RESULTS

3.1 *Fully Constrained and Unconstrained Transformation*

Fig.1 shows the $\triangle L-T$ and $\triangle R-T$ plots of spring 1. The solid lines represent the results under zero-stress (unconstrained) and the dashed lines show the result under zero-displacement (fully constrained) conditions. Under fully constrained conditions, the shape memory strain is completely suppressed and the $\triangle L-T$ plot is a horizontal line. Under unconstrained conditions, the transformation process is characterized by the corresponding $\triangle L-T$ or $\triangle R-T$ plots.

Following the same definitions of the transformation temperatures as described in the paper by Li *et al* [6], the transformation temperatures under unconstrained conditions determined by electrical resistivity measurements: $M_s=304.8$ K, $M_f=294.6$ K, $A_s=304.8$ K and $A_f=310.8$ K. On the other hand, the transformation temperatures determined by length change measurements were: $M_s'=306$ K, $M_f'=298.2$ K, $A_s'=307.2$ K and $A_f'=311.4$ K. The transformation temperatures determined by the latter method are higher than those determined by the former method.

Fig.1 also shows that the response of the shape memory deformation to the external restraining stress is significantly different from that of the electrical resistivity during transformation. Under fully constrained conditions, the shape memory deformation is completely suppressed whereas significant changes in electrical resistivity still occur during temperature cycling. In the latter case, the effects of the restraining stress are

slight reductions in the transformation temperatures and a narrower hysteresis loop.

In order to gain further insight into the experimental results mentioned above, we designed the thermomechanical treatment schedule shown in Fig.2 on the spring specimen. The thermomechanical treatment schedule is outlined in the following:

STEP 1 A→B ($\triangle L=0$, $L=L_0$), heating from room temperature to 330 K under full constraint;

STEP 2 B→C ($\triangle T=0$, $T=330$ K), removal of the constraint at constant temperature above A_f';

STEP 3 C→D ($\triangle L=0$, $L=L_{max}$), cooling from 330 K to room temperature under full constraint.

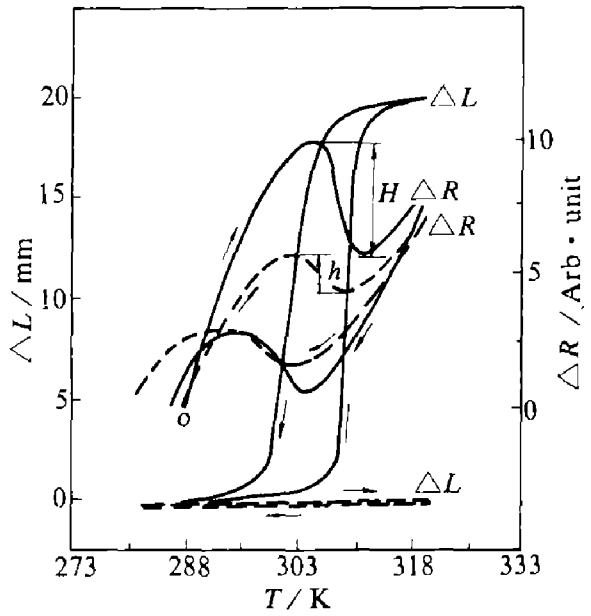

Fig. 1 The $\triangle L-T$ and $\triangle R-T$ curves of spring 1 under unconstraint and full constraint.

Solid line—unconstrained dashed line—Full constrained

Fig.3 shows the X-ray diffractometer traces of the spring specimen at four conditions (*A*, *B*, *C* and *D*), which correspond to the four conditions indicated in Fig.2. At the beginning, with no constraint and at room temperature, the specimen was found to contain almost 100% martensite (Fig.3(A)). When the temperature was raised to 330 K (above A_f') under full constraint, only a partial phase transformation to the parent phase (*P*) occurred (Fig.3(B)). This was not due to the phenomenon of martensite stabilization, because 100% parent phase could be obtained after the removal of the constraint (Fig.3(C)). In later discussion, it is proposed that the martensite retained in (B) is directly related to shape recovery, $\triangle L$. When the temperature was reduced to room temperature under constraint, it was found that only partial parent phase transformation to martensite occured (Fig.3(D)). Complete P→M transformation was not obtained.

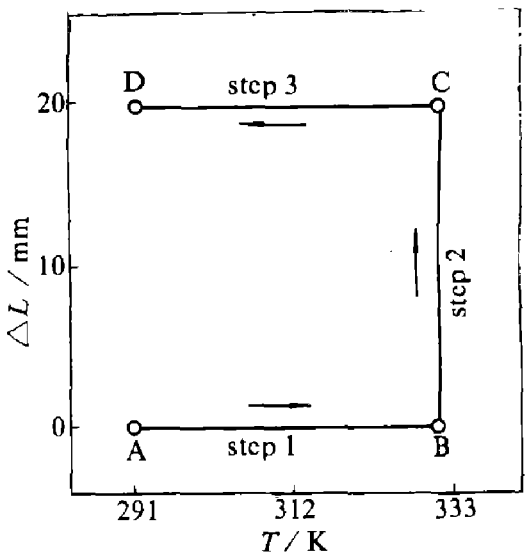

Fig.2 The experimental program for in-situ X-ray diffraction under constraint.

We can infer from these results that there is a part of the parent / martensite transformation which is responsible for the shape memory strain in TWSM. Under full constraint, the shape memory strain and the corresponding" memory strain transformation" are suppressed. However, there is another part of the transformation which can still occur under full constraint. This part of the transformation does not result in a macroscopic change in shape and is termed a self accommodating transformation.

Assuming that the electrical resistivity change, $\triangle R$, is proportional to the transition volume fraction, the relative proportions of the two types of transformations may be estimated from the

magnitudes of $\triangle R$. Referring to Fig.1, the volume fraction, V_m, connected with the memory strain transformation can be estimated from $V_m \approx 1-(h/H)$, which gives a value of about 65%. (Where H and h are the total magnitude of $\triangle R$ during $M \rightleftharpoons P$ transformation on heating under unconstrained and fully conditions constrained respectively).

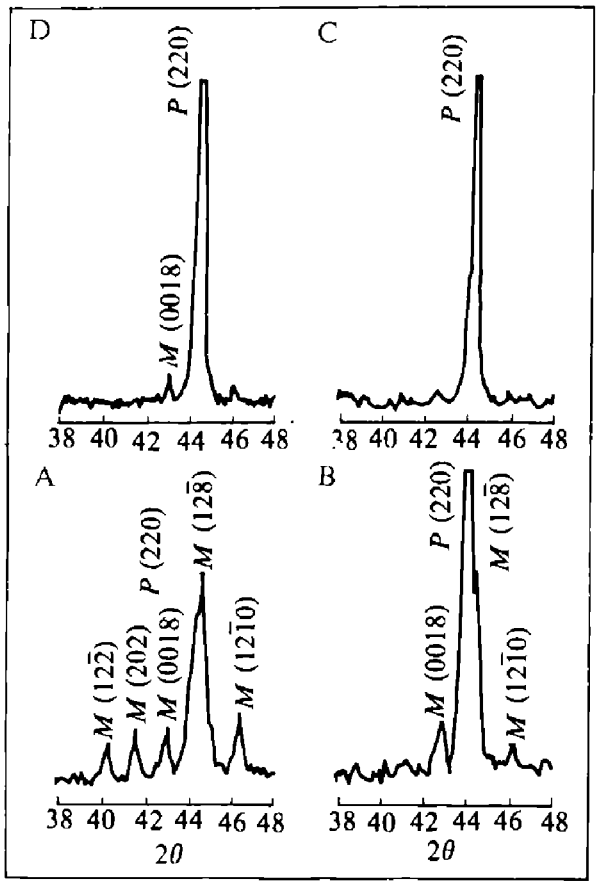

Fig.3 The X-ray diffraction patterns of spring 1 under differential constrained conditions.

3.2 *The Influence of Stress on Memory Strain Trans- formation*

A series of $\triangle L-T$ loops under different compression loads were determined using spring 2 and three typical loops are shown in Fig.4. As expected, the overall memory strain decreases with increasing compression load. The $\triangle L-T$ loop is shifted towards higher temperatures upon compression loading. Since the compression suppresses transformation on heating but promotes transformation on cooling, the loop becomes more asymmetric as the compression load is increased.

The effect of shear stress in the surface of an alloy wire, τ, on the transformation temperatures is given in Fig. 5.τ is calculated by[11]:

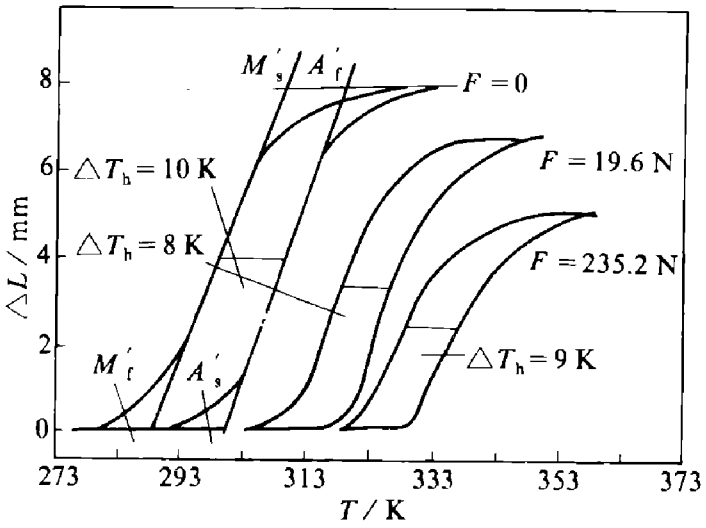

Fig. 4 The influence of compression on the $\triangle L-T$ loop of spring 2.

$$\tau = k\frac{8FD}{\pi d^3} \quad (1)$$

where F is the compression load (9.8066 N); $k=[C/(C-1)]+[1/(2C)]$; $C=Dd$; D is the average diameter of the spring and d is the diameter of the alloy wire.

The transformation temperatures vary linearly with τ and have almost the same slope in Fig.5. Taking the width of the loop at half height, $\triangle T_h$, as a measure of hysteresis, it can be seen from Fig. 4 that the effect of shear stress on hysteresis is small.

4 DISCUSSION

In polycrystalline samples, 100% preferential re-orientation is not likely to occur even after training. Thus, the variants are likely to consist of two types. Variant 1 is highly oriented and is responsible for TWME during transformation; Variant 2 is self-accommodating and does not contribute to macroscopic shape change. The

relative proportions of these two variants depend on a number of factors, e.g., alloy species, grain size and training process. The experimental results obtained in this investigation provide supporting evidence of the existence of these two types of variants.

Since the transformation of variant 1 is responsible for the macroscopic shape change, it is particularly sensitive to the applied stress. When the shape memory alloy is forced by an applied stress to such an extent that the memory strain is completely suppressed, the corresponding transformation of variant 1 is also suppressed. However, the transformation of variant 2 can occur.

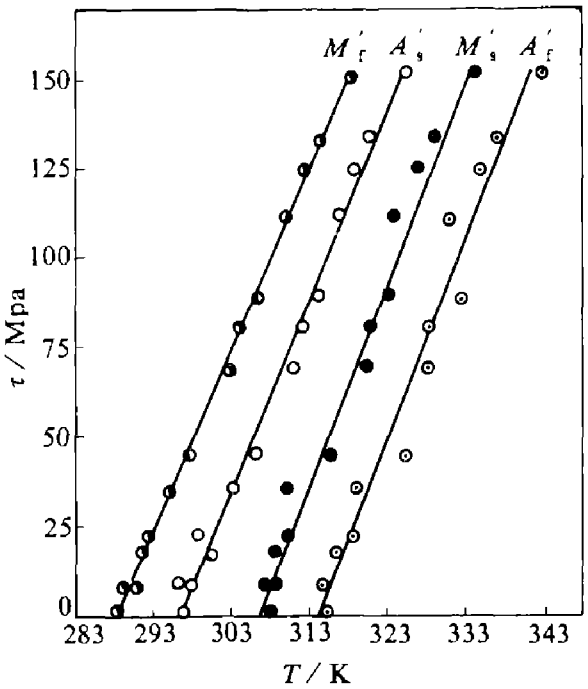

Fig. 5 The effect of shear stress on the transformation temperatures of oriented variant

Thermoelastic martensitic transformation is a first-order transformation, and the process of variant growth can be considered to be the motion of phase interfaces. Following Olson and Cohen[12], the thermoelastic balance is given by

$$-\triangle G_{ch}+2\triangle G_{el}=-\triangle G_{fr}$$

on cooling (2)

$$\triangle G_{ch}+2\triangle G_{el}=\triangle G_{fr}$$

on heating (3)

where G's are in absolute values. $\triangle G_{ch}$ is the difference in Gibbs free energy. $\triangle G_{el}$ is the stored elastic strain energy. The elastic strain energy stored in the forward transformation will be released in the reverse transformation and will assist the reversion back to the parent. Hence, it has a major effect on the transformation equilibrium temperatures. $\triangle G_{fr}$ is an irreversible energy dissipation leading to transformation hysteresis[13,14].

From the above discussion, $\triangle G_{el}$ should consist of two parts:

$$\triangle G_{el}=\triangle G^1_{el}+\triangle G^2_{el} \quad (4)$$

where $\triangle G^1_{el}$ and $\triangle G^2_{el}$ are the elastic strain energies of the oriented and the accommodating variant respectively. The interfacial area of the oriented variant is likely to be smaller than that of the accommodating variant due to orientation and preferential growth. Thus, $\triangle G^1_{el}$ is likly to be less then $\triangle G^2_{el}$[15]. From the thermodynamic relationships given in equations (2) and (3), the transformation temperatures of the oriented variant are expected to be higher than those of the accommodating variant. This is confirmed by the experimental results which show that the $\triangle L-T$ loop is shifted to the high temperature side compared with the $\triangle R-T$ loop (Fig.1.).

In the present expreiment, the comperssive force, F, promotes the $P\rightarrow M$ transformation and inhibits the reverse transformation. The interface equilibrium equations (2) and (3), can be written as

$$-\triangle G_{ch}-F\triangle L+2\triangle G_{el}=-\triangle G_{fr}$$

on cooling (5)

$$\triangle G_{ch}-F\triangle L+2\triangle G_{el}=-\triangle G_{fr}$$

on heating (6)

The effect of the term $F\triangle L$ increases the transformation temperatures. Consequently the $\triangle L-T$ loops are shifted towards higher temperatures as the compressive force increases (Fig.4). On the other hand, the hysteresis, represented by $\triangle T_h$ in the $\triangle L-T$ loops, is not significantly change, suggesting that the frictional work done, a dynamic property of the interfacial motion, is

unaffected by F.

5 CONCLUSIONS

(1) The martensitic variants in two way shape memory alloys may be classified into a preferred orientation variant and a self-accommodating variant. Macroscopic shape change in the TWSM is attributed to the transformation of the oriented variant. The self accomodating variant does not contribute to the overall macroscopic memory strain;

(2) The oriented variant is sensitive to external stress. Externally applied stress may promote or inhibit the transformation of the oriented variant, thereby affecting the transformation temperatures, but has no essential effect on the transformation of the accommodating variant;

(3) The interfacial area of the oriented variant is likely to be smaller than that of the accommodating variant due to orientation and preferential growth. Thus, the transformation temperatures of the oriented variant are expected to be higher than those of the accommodating variant. This is confirmed by the experimental results which show that the length change vs temperature is shifted to the high temperature side compared with the electrical resistivity vs temperature loop.

REFERENCES

1 Dunstan, P S. *et al.* J. Mater. Sci., 1986, 21(6): 1637.
2 Ketley, C *et al.* In: Proc Inter Synp SMA–86, China Academic, Beijing, 1986. 89.
3 Lin, G M *et al.* scripta Metall. Mater., 1990, 24(8): 1587.
4 Madangopal, K *et al.* Scripta Metall., 1988, 22(10): 1593.
5 Edo, S. J Mater Sci, 1989, 24(11): 3991.
6 Lu, Li *et al.* Scripta Metall, 1988, 22(9): 1435.
7 Xu, H *et al.* Scripta Metall. Mater, 1991, 25(7): 1507.
8 Jardine, A P. J Mater Sci, 1989, 24(7): 2587.
9 Perkins, J *et al.* Metall Trans, 1984, A15(2): 313.
10 Lin, G M *et al.* Actal Metall Sinica, 1989, 25(6): A400.
11 Suguki, In-ichi. Industry Materials (Japanese), 1983, 31(1): 72.
12 Olson, G B *et al.* Scripta Metall, 1975, 9(7): 1247.
13 Delacy, L *et al.* In: Proc of ICOMAT–86, Nara, Japan, 1986. 926.
14 Ortin, J *et al.* Acta Metall, 1988, 36(8): 1873.
15 Sulgbrenner, R J *et al.* Acta Metall, 1979, 27(5): 739.